Ammonium Polyphosphate/Melamine Cyanurate Synergetic Flame Retardant System for Use in Papermaking

Wenguang Yang,[a] Fei Yang,[a,b] Rendang Yang,[a] and Bin Wang [a,b,*]

A new synergetic flame retardant system (SFRS) using ammonium polyphosphate/melamine cyanurate (APP/MCA) core-shell particle was synthesized and applied to papermaking. Cationic polyacrylamide (CPAM) was added to improve the adsorption of SFRS in pulp. Higher amounts of SFRS led to higher adsorption by pulp. Handsheets were produced with different amounts of SFRS. Thermal gravimetric analysis (TGA) and limiting oxygen index (LOI) were employed to test fire retardation in these handsheets. TGA and LOI results showed that this new core-shell SFRS is an effective flame retardant that improves the thermal stability of handsheets.

Keywords: MCA; Ammonium polyphosphate; Melamine cyanurate; APP; APP/MCA; Flame retardation

Contact information: School of Light Industry and Food Sciences, South China University of Technology, Guangzhou, 510640, China; b: Key Lab of Paper Science and Technology of Ministry of Education, Qilu University of Technology, Jinan, Shandong Province 250353, China;
** Corresponding author: febwang@scut.edu.cn*

INTRODUCTION

The rapid development of heat-resistant materials, reinforcement materials, and impact-resisting materials has led to an increasing demand for their high thermal stability (Sun *et al*. 2012; Yokota *et al*. 2013). Additionally, materials that are lightweight, highly flexible, low cost, and easily recovered are desirable. Plant fibers are commonly used to make paper that has these properties.

The main components of fibers are cellulose, hemicellulose, and lignin (Arnold *et al.* 1943). These flammable substances directly affect the thermal properties of paper (Lee *et al*. 2002). Hence, the flammability of fibers limits their application in making paper.

Melamine cyanurate (MCA) is a new type of environmental flame retardant (Bielejewska *et al.* 2001). When MCA is heated, sublimation easily occurs, and it decomposes into gaseous NH_3 and CO_2 (Casu *et al.* 1997). The formation of protective covers by these non-flammable gases automatically segregates heat sources and the target object; thus, air is isolated from the target object. This physical separation method allows MCA to be successfully used in the rubber industry (Gijsman *et al.* 2002; Braun *et al.* 2008). An important drawback of MCA is its poor solubility and absorptivity. When MCA is added to pulp suspensions, MCA particles drain away with water. This not only wastes MCA but also leads to whitewater recycling problems.

Ammonium polyphosphate (APP) has been used as a paper flame retardant for decades (Chiu and Wang 1998). Unlike MCA, high temperature weakens the stability of APP, causing its decomposition to polyethylene and phosphoric acid (Bourbigot *et al.* 1995). These molecules are strong desiccants that absorb water from plant fibers and then

form a compact carbide layer on the fiber surface, which separates oxygen and heat sources from the fibers (Alongi *et al.* 2012; Carosio *et al.* 2012). The inherent defects of APP are its water insolubility; high molecular weight of APP makes it insoluble in water (Shen *et al*. 1969). If APP is directly introduced into fiber, the resulting paper has several problems, including poor hygroscopicity.

This study details an adsorptive method that overcomes these problems by forming a fire-retardant layer on the pulp surface. A new synergetic flame retardant system (SFRS) was designed and synthesized (Fig. 1). Zeta potential was measured as SFRS adsorbed on the fibers surface through electrostatic interaction. Pulp with different amounts of SFRS was used to make handsheets that were structurally characterized by scanning electron microscopy (SEM) and X-ray diffraction (XRD). The thermal and flame-resistant properties of handsheets were also analyzed by thermal gravimetric analysis (TGA) and limiting oxygen index (LOI), and the SFRS handsheets were compared to the original handsheets at elevated temperatures. Finally, the SFRS handsheets and the corresponding effects on physical properties were investigated.

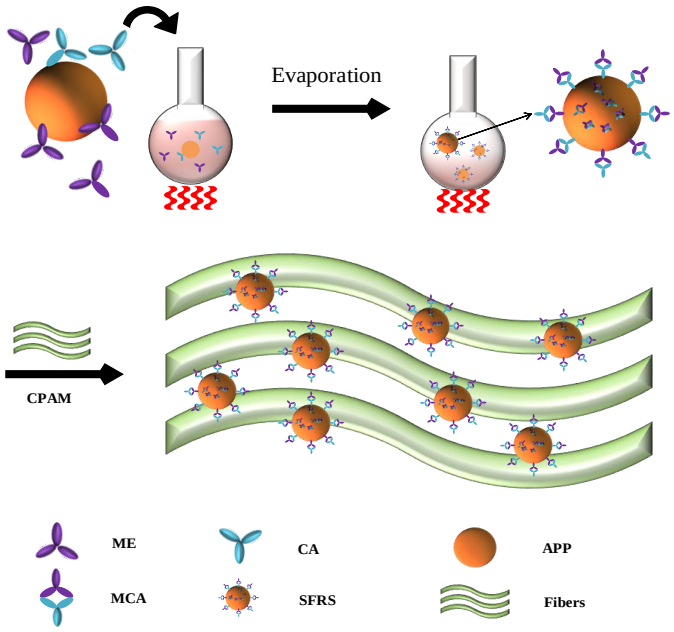

Fig. 1. Procedure for the formation of the core-shell APP/MCA synergetic flame retardant system

EXPERIMENTAL

Materials

Bleached sulfate bamboo pulp and ammonium polyphosphate (polymerization degree ≥ 1500) were kindly supplied by Lvyuan Co. Ltd. (Guangdong, China). Melamine (purity > 99%), alkali salt (purity > 99%), ethanol solution (purity > 99.9%), cyanuric acid (purity > 99%), and melamine cyanurate (purity > 99%) were purchased from Aladdin Chemistry Co. Ltd. (China). The melamine (ME) and cyanuric acid (CA) were limited to ≤ 2.0 μm by screening, and the APP diameter ranged from 10.0 to 20.0 μm. Cationic polyacrylamide (CPAM) was provided by Hengfeng Chemical Co. Ltd. (Zhejiang, China) and had the following properties: substitution degree: 0.2, molecular weight: 8 million g/mole, positive charge: 1.53 meq/g.

Preparation of the APP/MCA Synergetic Flame Retardant System

A solution of absolute ethanol (250 mL) was heated at 78 °C with a heating mantle in a 500-mL three-necked round-bottomed flask for 15 min with vigorous stirring. A condenser was utilized to prevent solvent evaporation. After boiling, 10.0 g of ME, 10.0 g of CA, 2.0 g of APP, and 0.2 g of alkali salt were added to the ethanol solution and stirred for 4 h at 78 °C. The products were decanted into a filter, washed three times each with deionized water and absolute ethanol, and dispersed uniformly into solution *via* sonication.

Handsheet Preparation and Testing

Bleached sulfate bamboo pulp (dry weight 3.14 g) was fully dispersed in 1000 mL of water by a disintegrator at 3,000 rpm. The SFRS was added to the fiber suspension to different final concentrations (5%, 10%, 15%, 20%, 25%, and 30%) with stirring. CPAM (0.05%) was added to the slurry pulp to give the system a positive charge. To track electrochemical properties, the zeta potential of the untreated slurry pulp and pulp-SFRS were measured using a SZP-06 system zeta potential analyzer (Mütek, Germany). Handsheets with a grammage of 100 g/m^2 (except for SFRS) were prepared on a sheet-making apparatus (PTi LLC, IL, USA). Wet handsheets were dried at 102 °C and 1000 kPa pressure. The phosphorus content was measured by an atomic absorption spectrometer (Z–2000, Hitachi, Japan) to confirm the adsorption of SFRS to pulp. The handsheets were stored in a controlled environment (23 ± 1 °C, 50 ± 1% RH) for 24 h before testing. The handsheet burst index (L&W CE180), tearing strength (L&W 009), and ash contents were measured following TAPPI standard T 211 (Alfaro *et al.* 2009). To measure thermal properties, these tests were also applied to handsheets heated at 200 °C for 24 h.

Transmission Electron Microscope (TEM)

The microstructure of SFRS (APP/MCA) was observed by a JEM-2100F transmission electron microscopy (TEM) (JEOL, Japan) at an accelerating voltage of 200 kV. The sample was dispersed in water and placed on a copper grid coated with ultrathin carbon film.

Scanning Electron Microscopy (SEM)

SEM images were obtained using a Merlin Scanning Electron Microscope (ZEISS, Oberkochen, Germany) at an acceleration voltage of 25 kV. The samples were mounted on an aluminum stub using double-sided tape and coated with Au (JEOL JFC- 1600 Auto Fine Coater, Japan) under vacuum prior to analysis.

Fourier Transform Infrared Spectroscopy (FTIR)

FT-IR spectra for the handsheets were recorded with a Vertex 33 (Bruker, Germany). The samples were mixed and ground with KBr for IR measurements within the frequency range of 400 to 4000 cm^{-1}.

Thermal Gravimetric Analysis (TGA)

Thermal gravimetric analysis of the handsheets was performed on a Netzsch TG209 Jupiter Thermal Analysis System (TA Instruments, USA) with a fixed heating rate of 10 °C/min. Approximately 10 mg of sample was used in each test. The temperature range was 25 to 600 °C, and the flow rate was 50 mL/min in a nitrogen environment.

Limiting Oxygen Index (LOI)

The LOI method was used to measure the ignitability of the handsheets. The handsheets were measured using a FTT0078 oxygen index meter (Fire Testing Technology, England) strictly according to the standard oxygen index test (Lijie *et al.* 2012). The LOI values were the average of five tests for each sample.

RESULTS AND DISCUSSION

TEM and SEM Analysis of SFRS and Its Reaction Mechanism

TEM and SEM were carried out to investigate the morphology of SFRS. As shown in Fig. 2A and 2B, SFRS exhibits a spherical granular shape (Fig. 2B), and shows a uniform core-shell structure (Fig. 2A). Melamine combined with cyanuric to form melamine cyanurate acid through hydrogen bond (Bielejewska *et al*. 2001). Nitrogen atoms of melamine contained a lone pair electrons in 2s orbit which made hydrogen easily be captured by melamine (Zhang 2010). But steric hindrance of heterocyclic nitrogen was stronger than amino nitrogen. Therefore the mainly reaction D was well-founded. Nitrogen-atoms of melamine got H^+ from HCO_3^- and obtained the ability for electrically attract O^-–P– of ammonium polyphosphate (Jahromi *et al.* 2003). In this way, MCA acted as the shell surrounded app and app acted as the core. The core-shell structure was formed and is shown in Fig. 2 A and 2B.

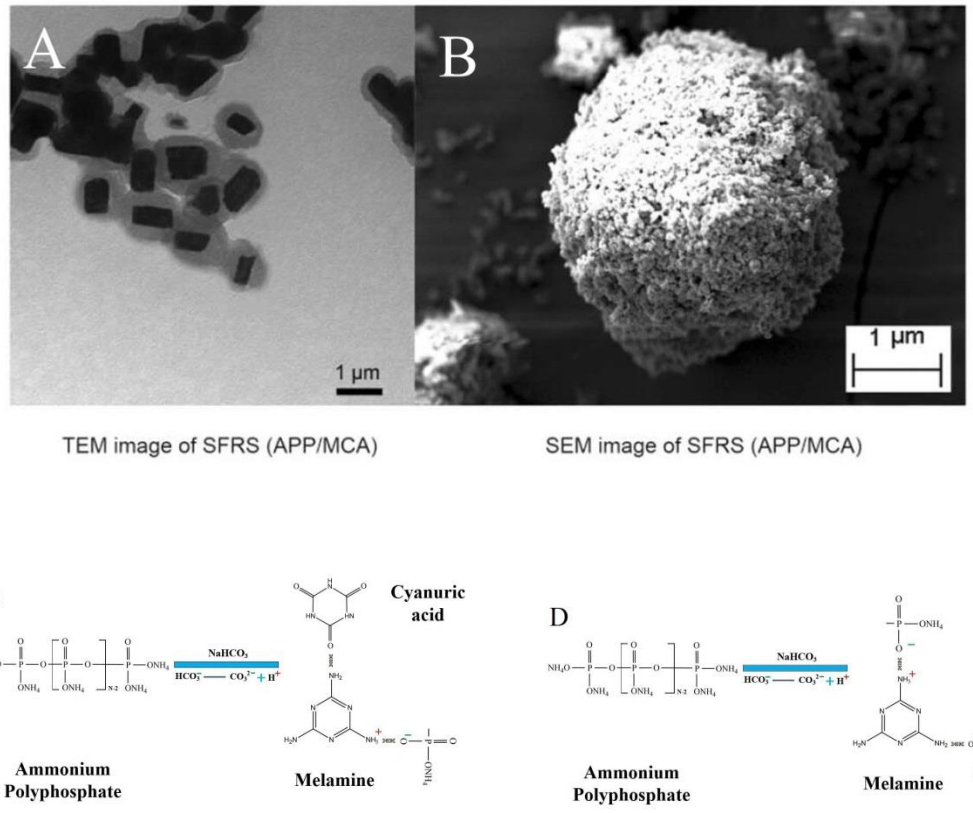

Fig. 2. The morphology of APP/MCA (SFRS) and reaction mechanism

Fourier Transform Infrared Spectroscopy for SFRS and Handsheets

The structures of APP, APP/MCA (SFRS), pulp, and pulp with SFRS were analyzed by FTIR (Fig. 3). In the MCA spectrum, the peaks at 3384 and 3224 cm^{-1} corresponded to -NH symmetric and asymmetric stretching vibration, respectively. The peaks at 1533, 1440, and 770 cm^{-1} represented the triazine ring and outside bending vibration of the ring in MCA (Braun and Schartel 2008). When APP was introduced to MCA, new peaks appeared at 1019 and 824 cm^{-1}. These peaks were attributed to symmetric vibration of PO_2, PO_3, and P–O–P stretching from APP (Levchik *et al.* 1995). The peak at 3033 cm^{-1} indicated the N–H stretching vibration of MCA. The results suggested the successful synthesis of SFRS.

In pulp, the absorption peak of OH groups were located at 3500 cm^{-1}. The vibration absorption peak at 2900 cm^{-1} was attributed to the C–H stretching vibration. Compared with untreated pulp, pulp–SFRS exhibited additional bands at 1533 and 1440 cm^{-1}. This result verified that APP/MCA had been adsorbed on the pulp surface.

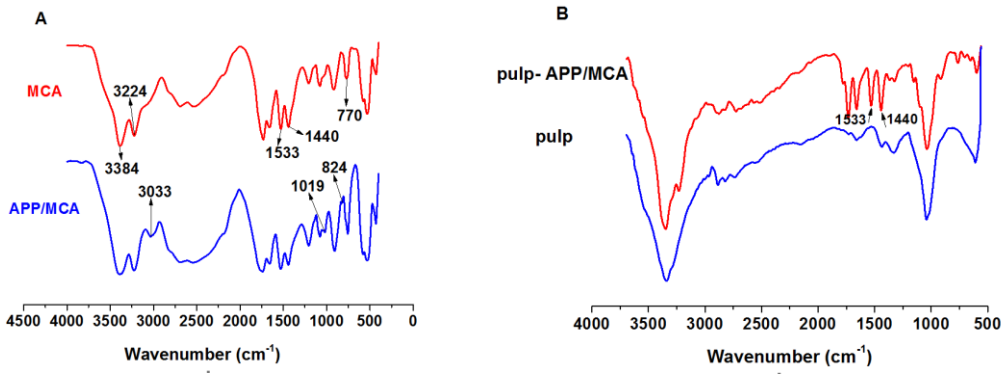

Fig. 3. FTIR spectra of MCA and SFRS (A) or pulp and pulp–SFRS (B)

Adsorption Mechanism

The morphology of handsheets made from pulp or pulp-SFRS was examined by SEM (Fig. 4a). Untreated pulp fibers showed a smooth and uniform surface (sample 0), with some apparent folds caused by drying during the papermaking process. Scanning electron microscopy of pulp-SFRS (sample 6) showed that SFRS particles were successfully adsorbed on the surface of pulp fibers. The existence of phosphorus (P) in pulps also confirmed that adsorption was successful.

Zeta potential was measured to examine the interaction(s) between pulp fiber and SFRS. For samples 0 through 6 (Table 1), the zeta potential of pulp changed from -40.1 mV to -24.2 mV as the SFRS dosage increased (Fig. 5). However, the zeta potential changed dramatically from negative to positive values after the addition of 0.05% CPAM. This shift reflected a neutralization of components that contribute to an overall negative charge on the pulp surface, such as glucuronic acid and polar hydroxyls. CPAM changes the pulp suspension to a positive charge, which lowers the zeta potential.

As illustrated in Fig. 1, pulp fibers are homogeneously dispersed in the pulp suspension. The addition of APP/MCA (SFRS) reduced the zeta potential, resulting in an electrostatic attraction. Although static adsorption was achieved between MCA and pulps (Fig. 4(b)), the fact is that it only plays a small contribution. CPAM is also needed to link SFRS onto the pulp surface. The adsorption of SFRS on the fiber surface is limited by the turbulent conditions of the papermaking process. The link between SFRS and CPAM also

resulted in a dramatically higher phosphorus content in pulp-SFRS after the addition of 0.05% CPAM (Table 1).

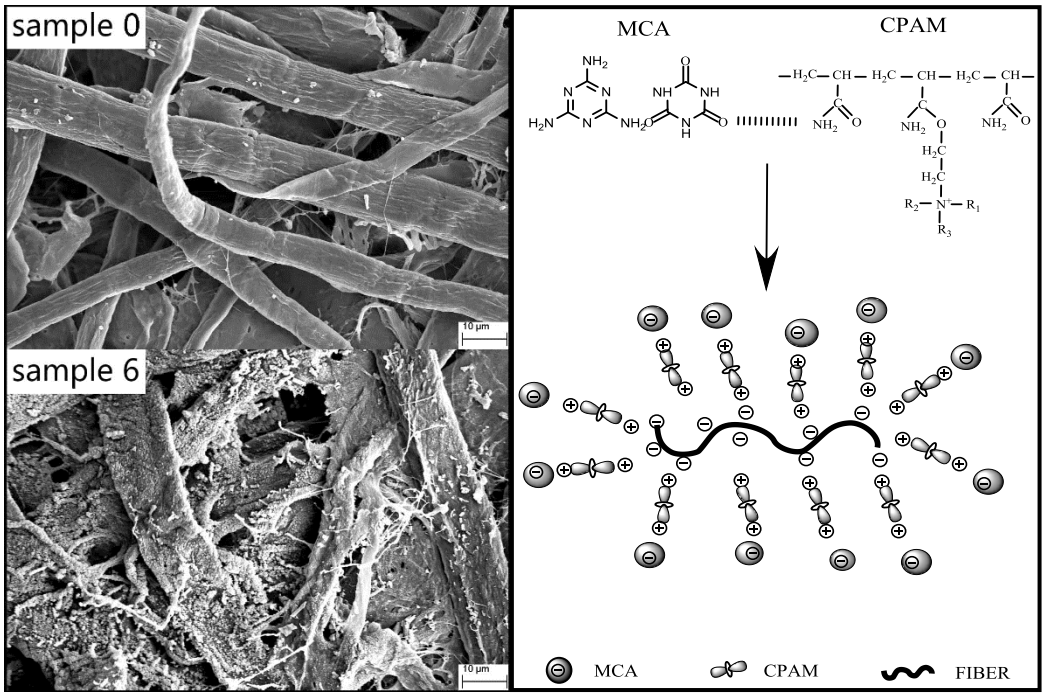

Fig. 4. (a) SEM image of sample 0 and 6 handsheets; (b) a schematic diagram of CPAM facilitating MCA adsorption on fibers

Thermal Gravimetric Analysis

The zeta potential and morphology data showed that APP/MAC adsorbs on the surface of pulp. To further demonstrate the thermodynamic properties of pulp-SFRS, thermal gravimetric analysis (TGA) was utilized for MCA, APP/MCA, handsheets, and handsheets with APP/MCA (Fig. 6). The mass-loss regions of the MCA are from 316 to 400 °C. MCA decomposes into NH_3 and CO_2 in this temperature range (Zhang *et al.* 2008). APP/MCA has two mass loss stages. The first stage is at 280 to 320 °C, mainly caused by the release of NH_3 and water from APP. During heating, APP first decomposes to polyphosphoric acid and then is further dehydrated (Lin *et al*. 2011). The second stage is the same as MCA, which occurs from 320 to 400 °C (Wu *et al*. 2008).

Pulp decomposed in two steps. The first mass-loss regions for the pulps were between 25 and 200 °C, when water was released from the pulps. The second mass-loss range was 200 to 400 °C and was due to the depolymerization of hemicellulose and cellulose. The ash content of pulp fiber was increased by the addition of APP/MCA. The first degradation stage occurred earlier (Fig. 6(d)) than in handsheets (Fig. 6(c)). The mass loss peak at 313 °C corresponded to the decomposition of APP/MCA. The second decomposition stage occurred at 372.55 °C, which was 50 °C higher than the second stage (342.05 °C) in handsheets (Fig. 6(c)). This shift was probably due to the slow combustion of APP/MCA.

The thermal gravimetric analysis suggested that APP interacts with pulp during thermal degradation. The formation of a phosphorus layer could protect the pulp against

heat. However, the protective layer can break down and form a compact char on the material surface (Siat *et al.* 1997; Meng *et al.* 2009).

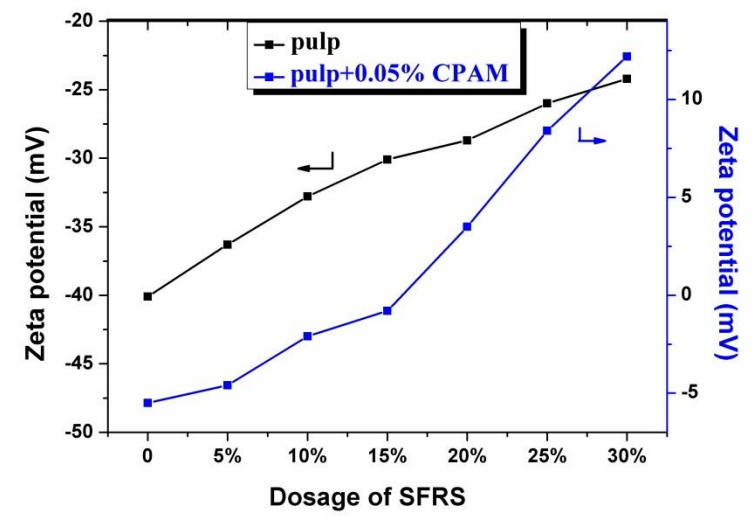

Fig. 5. Zeta potential of pulp and pulp with 0.05% CPAM at varying concentrations of SFRS

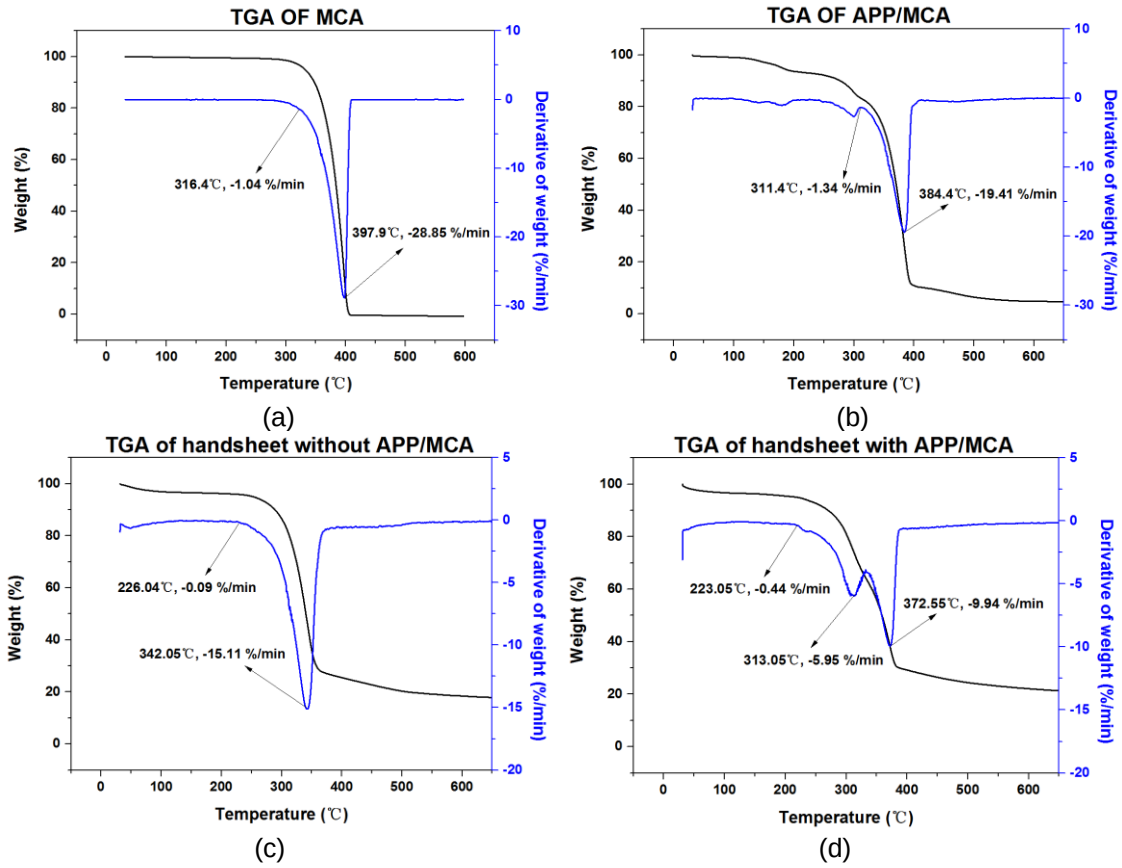

Fig. 6. Thermal gravimetric analysis of (a) MCA; (b) APP/MCA (SFRS); (c) sample 0; (d) APP/MCA handsheet (sample 6)

Influence of SFRS Content on Physical Properties of Handsheets

The influence of various amounts of SFRS on the physical properties of handsheets is shown in Table 1. The ash content of handsheet samples increased as the SFRS increased; APP decomposes into polyethylene and phosphoric acid, which can build a dense layer to prevent the access of oxygen and heat source to the surface of fiber. The burst index and tensile index of handsheets decreased slightly as the addition of SFRS increased (Table 1, columns marked A).

Table 1. Influence of SFRS on Handsheet Physical Properties

Handsheet Samples	SFRS (%)	Burst Index ($kPam^2/g$)		Tensile Index (Nm/g)		Ash (%)	Phosphorus Content[C] (%)
		A	B	A	B		
0	0	11.91	5.39	146.25	82.22	0.62	0.10
1	5%	11.64	7.87	140.86	97.47	0.70	0.57
2	10%	11.22	8.68	137.58	102.32	0.84	0.68
3	15%	10.50	8.81	131.71	109.38	0.98	0.95
4	20%	10.23	8.94	128.54	115.26	1.12	1.36
5	25%	10.14	9.32	125.39	116.28	1.18	2.34
6	30%	10.03	9.44	124.61	118.03	1.21	2.89

A: Handsheets without thermal treatment
B: Handsheets exposed to 200 °C for 24 h

With the addition of 30% SFRS, the burst index and the tensile index decreased by 15.79% and 14.80% than the raw paper, respectively. Thus, the addition of SFRS have little effect on the physical properties of handsheets (Camarero *et al.* 2004). The burst index and the tensile index only decreased by 5.88% and 5.28%, respectively, after exposure at 200 °C for 24 h (Table 1, columns marked B). However, the burst index and tensile index of handsheets without any additives decreased by 54.74% and 43.78%, respectively. This result proved that SFRS improved the thermal stability of handsheets.

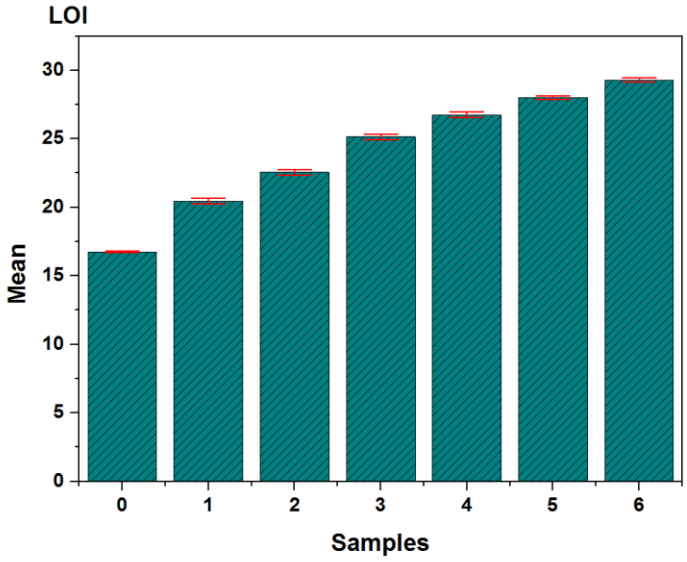

Fig. 7. Limiting oxygen index of handsheet samples 0-6 with varying SFRS concentration

Limiting Oxygen Index Analysis

The limiting oxygen index (LOI) method was used to determine the flame retardant properties of handsheets (Fig. 7). Because pulp fibers are very flammable materials, the LOI of handsheets without any additives was 16.7. With addition of 30% APP, the LOI reached 29.3. Hence, the presence of APP effectively enhanced flame retardation in handsheets. Furthermore, LOI increased as the addition of APP increased.

CONCLUSIONS

1. An ammonium polyphosphate/melamine cyanurate (APP/MCA) synergetic flame retardant system was successfully synthesized. The core-shell structure of the APP/MCA (SFRS) was formed with MCA acting as shell surrounded app and app acted as the core. With the addition of CPAM, synergetic flame retardant system (SFRS) particles adsorbed on the surface of fibers through electric attraction.
2. During heating the handsheets, the APP/MCA played a role in resisting high temperature. MCA firstly decomposed into ammonia and CO_2 which could dilute the oxygen in air and isolated the heat from fire. When MCA was expended, APP took over the dominate role in SFRS. It decomposed into phosphoric acid, and then formed a compact carbide layer on the fiber surface to isolate oxygen and inhibit pyrolysis. These physicochemical changes could greatly enhance the flame retardant efficiency of fibers and improve the thermal stability of handsheets.

ACKNOWLEDGMENTS

The authors are grateful for the support of the Natural Science Foundation of Guangdong Province (2015A030310369 & 2015A030313221) and the Foundation (No. 0308031363 & 0308031367) of Key Laboratory of Pulp and Paper Science and Technology of Ministry of Education (Qilu University of Technology).

REFERENCES CITED

Alongi, J., Carosio, F., and Malucelli, G. (2012). "Layer by layer complex architectures based on ammonium polyphosphate, chitosan and silica on polyester-cotton blends: Flammability and combustion behaviour," *Cellulose* 19(3), 1041-1050. DOI: 10.1007/s10570-012-9682-8

Arnold, H. W., Dorough, G. L., and Latham, G. H. (1943). "Coated cellulosic material," U.S Patent No. 2334236.

Bielejewska, A. G., Marjo, C. E., Prins, L. J., Timmerman, P., de Jong, F., and Reinhoudt, D. N. (2001). "Thermodynamic stabilities of linear and crinkled tapes and cyclic rosettes in melamine-cyanurate assemblies: A model description," *Journal of the American Chemical Society* 123(31), 7518-7533. DOI: 10.1021/ja010664o

Bourbigot, S., Le Bras, M., Delobel, R., Bréant, P., and Trémillon, J. (1995). "Carbonization mechanisms resulting from intumescence-part II. Association with an

ethylene terpolymer and the ammonium polyphosphate-pentaerythritol fire retardant system," *Carbon* 33(3), 283-294. DOI: 10.1016/0008-6223(94)00131-I

Braun, U., Bahr, H., Sturm, H., and Schartel, B. (2008). "Flame retardancy mechanisms of metal phosphinates and metal phosphinates in combination with melamine cyanurate in glass-fiber reinforced poly(1,4-butylene terephthalate): The influence of metal cation," *Polymers for Advanced Technologies* 19(6), 680-692. DOI: 10.1002/pat.1147

Camarero, S., Garcıa, O., Vidal, T., Colom, J., del Rıo, J. C., Gutiérrez, A., Grasd, J. M.,Monjea, R., Martíneza, M. J., and Martınez, Á. T. (2004). "Efficient bleaching of non-wood high-quality paper pulp using laccase-mediator system," *Enzyme and Microbial Technology* 35(2), 113-120. DOI: 10.1016/j.enzmictec.2003.10.019

Carosio, F., Alongi, J., and Malucelli, G.. (2012). "Layer by layer ammonium polyphosphate-based coatings for flame retardancy of polyester–cotton blends," *Carbohydrate Polymers* 88(4), 1460-1469. DOI: 10.1016/j.carbpol.2012.02.049

Casu, A., Camino, G., De Giorgi, M., Flath, D., Morone, V., and Zenoni, R. (1997). "Fire-retardant mechanistic aspects of melamine cyanurate in polyamide copolymer," *Polymer Degradation and Stability* 58(3), 297-302. DOI: 10.1016/S0141-3910(97)00061-X

Chiu, S., and Wang, W. (1998). "Dynamic flame retardancy of polypropylene filled with ammonium polyphosphate, pentaerythritol and melamine additives," *Polymer* 39(10), 1951-1955. DOI: 10.1016/S0032-3861(97)00492-8

Gijsman, P., Steenbakkers, R., Fürst, C., and Kersjes, J. (2002). "Differences in the flame retardant mechanism of melamine cyanurate in polyamide 6 and polyamide 66," *Polymer Degradation and Stability* 78(2), 219-224. DOI: 10.1016/S0141-3910(02)00136-2

Jahromi, S., Gabriëlse, W., and Braam, A. (2003). "Effect of melamine polyphosphate on thermal degradation of polyamides: A combined X-ray diffraction and solid-state NMR study, " *Polymer*, 44(1), 25-37. DOI: 10.1016/S0032-3861(02)00686-9

Lee, S., Teramoto, Y., and Shiraishi, N. (2002). "Biodegradable polyurethane foam from liquefied waste paper and its thermal stability, biodegradability, and genotoxicity," *Journal of Applied Polymer Science* 83(7), 1482-1489. DOI: 10.1002/app.10039

Levchik, S. V., Camino, G., Costa, L., and Levchik, G. F. (1995). "Mechanism of action of phosphorus-based flame retardants in nylon 6. I. Ammonium polyphosphate," *Fire and Materials* 19(1), 1-10. DOI: 10.1002/fam.810190102

Lijie, W., Danlin, L., Xiaohua, H., Lixia, J., and Yang, Z. (2012). "Analysis and survey of oxygen index in polymer materials and its key factor," *Guangdong Chemical Industry* 39(7), 169-231.

Lin, H., Yan, H., Liu, B., Wei, L., and Xu, B. (2011). "The influence of KH-550 on properties of ammonium polyphosphate and polypropylene flame retardant composites," *Polymer Degradation and Stability* 96(7), 1382-1388. DOI: 10.1016/j.polymdegradstab.2011.03.016

Meng, X., Ye, L., Zhang, X., Tang, P., Tang, J., Ji, X., and Li, Z. (2009). "Effects of expandable graphite and ammonium polyphosphate on the flame-retardant and mechanical properties of rigid polyurethane foams," *Journal of Applied Polymer Science* 114(2), 853-863. DOI: 10.1002/app.30485

Shen, C. Y., Stahlheber, N. E., and Dyroff, D. R. (1969). "Preparation and characterization of crystalline long-chain ammonium polyphosphates," *Journal of the American Chemical Society* 91(1), 62-67. DOI: 10.1021/ja01029a013

Siat, C., Bourbigot, S., and Le Bras, M. (1997). "Thermal behaviour of polyamide-6-based intumescent formulations—A kinetic study," *Polymer Degradation and Stability* 58(3), 303-313. DOI: 10.1016/S0141-3910(97)00066-9

Sun, Y., Chen, Z., Noh, H., Lee, D., Jung, H., Ren, Y., and Amine, K. (2012). "Nanostructured high-energy cathode materials for advanced lithium batteries," *Nature Materials* 11(11), 942-947. DOI: 10.1038/nmat3435

Wu, K., Wang, Z., and Liang, H. (2008). "Microencapsulation of ammonium polyphosphate: Preparation, characterization, and its flame retardance in polypropylene," *Polymer Composites* 29(8), 854-860. DOI: 10.1002/pc.20459

Yokota, T., Kuribara, K., Tokuhara, T., Zschieschang, U., Klauk, H., Takimiya, K., Sadamitsu, Y., Hamada, M., Sekitani, T., and Someya, T. (2013). "Flexible low-voltage organic transistors with high thermal stability at 250 °C," *Advanced Material*, 25(27), 3639-3644. DOI: 10.1002/adma.201300941

Zhang, Y., Broekhuis, A. A., Stuart, M. C. A., Fernandez L., T., Fausti, D., Rudolf, P., and Picchioni, F. (2008). "Cross-linking of multiwalled carbon nanotubes with polymeric amines," *Macromolecules* 41(16), 6141-6146. DOI: 10.1021/ma800869w

Zhang Y., Liu Y., and Wang Q. (2010). "Synergistic effect of melamine polyphosphate with macromolecular charring agent novolac in wollastonite filled PA66," *Journal of applied polymer science*, 116(1): 45-49. DOI: 10.1002/app.31453

Article submitted: September 28, 2015; Peer review completed: November 16, 2015; Revised version received: December 27, 2015; Accepted: December 30, 2015; Published: January 20, 2016.
DOI: 10.15376/biores.11.1.2308-2318